Clim. Past Discuss., https://doi.org/10.5194/cp-2018-159
Manuscript under review for journal Clim. Past
Discussion started: 21 November 2018

Climate of the Past Discussions

Influence of the North Atlantic subpolar gyre circulation on the 4.2 ka BP event

Bassem Jalali[1], Marie-Alexandrine Sicre[1], Julien Azuara[2], Violaine Pellichero[1] and Nathalie Combourieu-Nebout[2]

[1]LOCEAN Laboratory, Sorbonne Universités (UPMC, Univ Paris 06)-CNRS-IRD-MNHN, Paris, France.

[2]Histoire naturelle de l'Homme Préhistorique (UMR 7194 CNRS), Département Homme et Environnement, Muséum national d'Histoire naturelle, Institut de Paléontologie humaine, France.

Abstract

The 4.2 ka BP event, spanning from ca 4200 to 3900 cal yr BP, has been documented in numerous archaeological data and continental archives across the northern hemisphere as an abrupt shift to dry and cold climate. However, data on synchronous ocean circulation changes are notably lacking thus preventing from getting a full insight into the physical mechanisms responsible for this climate deterioration. Here, we present two high-resolution sea surface temperature records from key locations in the subpolar gyre and off North Iceland in the vicinity of the polar front obtained from alkenone paleothermometry. Our data evidence a temperature dipole pattern in the subpolar North Atlantic between 4400-4100 yr BP, which combined with other paleoclimatic records from the North Atlantic/Euro-Mediterranean suggests a significant reduction of the subpolar gyre circulation possibly associated with atmospheric blocked regimes.

I. Introduction

Holocene rapid climate changes (RCCs) are century-long time intervals of enhanced high-latitudes cooling and tropical dryness (Mayewski et al., 2004, Wanner et al., 2011). The forcing mechanisms that trigger these RCCs are multiple and in many cases unclear (Wanner et al., 2014). Bond et al. (2001) suggested a relationship between these cold events and a reduction of the North Atlantic deep-water production (NADW) to explain their transmission around the Northern hemisphere. By examining 50 globally distributed proxy records, Mayewsky et al. (2004) concluded that RCCs result from natural external forcing (i.e. solar and volcanism) and interactions with internal variability (ocean-atmosphere dynamic). Wanner et al. (2011) highlighted the absence of a clear periodicity of the RCCs and the lack of spatio-temporal homogeneity of temperature and humidity conditions of these events. They also recognized that the early Holocene RCC known as the 8.2 event likely differed from late Holocene RCCs because of anomalously high freshwater forcing and insolation at the final stage of the deglaciation.

The 4.2 ka BP event, developing from 4200 to 3900 yr BP (Weiss, 2016), is one of the most widely documented RCCs. Considered as the second outstanding RCC after the 8.2 ka BP event in terms of magnitude and duration, it is often regarded as a boundary between the Middle and Late Holocene climate (Magny et al, 2013; Walker et al., 2012). It is notably known for being synchronous with a Megadrought in the Levant and the collapse of the Akkadian Empire and the Old Kingdom in Egypt, and further East of the Old Chinese cultures (Weiss and Bradley, 2001; Liu et al., 2012; Stanley et al., 2003). In the last decade, an increasing number of high-resolution proxy records has provided a more comprehensive description of this event (Weiss, 2016). In the Mediterranean region, climate reconstructions have highlighted a drastic reduction of precipitation and extreme climate conditions prevailing during this period (Magny et al., 2013; Fohlmeister et al., 2013; Zanchetta et al., 2016; Cheng et al., 2015; Ruan et al., 2016; Jalali et al., 2016; Finné et al., 2017; and references therein). According to Weiss (2015), a 30-50 % reduction of the precipitation delivered by the Mediterranean westerlies during the 4.2 ka BP event led to extreme dryness in the Middle East and Central Asia. The synthesis of Weiss (2016) further pointed out the weakening of major monsoon systems during this period. Evidences for Indian monsoon disruption comes from high-resolution speleothem and Lake Rara precipitation records (berkelhammer et al.,

2012; Dixit et al., 2014; Nakamura et al., 2016). Donges et al. (2015) also reported a weakening of East and South-West Asian summer monsoon resulting in pronounced dryness in northeastern China, Inner Mongolia and Australia. Finally, but not least, a drastic decline of precipitation was also observed over northern America (Booth et al., 2005; Fisher, 2008).

While the expression of the 4.2 ka BP event is evident in several paleoclimatic records all over the northern hemisphere, physical drivers of this climatic period are still not elucidated in part because of missing data from the ocean, the main water and heat reservoir on Earth. Based on continental hydroclimate records, Booth et al. (2005) proposed a La Niña -like pattern and warming in equatorial Atlantic Ocean to explain dry conditions in North America between 4.1 and 4.3 ka BP. Liu et al. (2014) suggested a transition from negative to positive Pacific North American (PNA)-like pattern as an alternative explanation. Transient simulations obtained from the Community Climate System Model (CCSM) of NCAR showed that while large-scale spatial pattern of the 4.2 and 8.2 ka BP events reproduce a pronounced cooling and precipitation reduction over the northern hemisphere the operating mechanisms are different (Ning et al. 2018, this issue). Cold and dry conditions during the 4.2 ka BP event would result from a weakening of the Atlantic meridional overturning circulation (AMOC) caused by direct insolation forcing while freshwater release in the Labrador Sea and subsequent AMOC collapse triggered the 8.2 ka BP event. Apart from different insolation conditions, these two RCCs experienced notably different volcanic forcing. Indeed, the absence of large volcanic eruptions (under strong solar activity) during the 4.2 contrasts with the intense volcanism of the 8.2 event (Kobashi et al., 2017).

In this paper, we present unprecedented high-resolution sea surface temperature records in the North Atlantic obtained from alkenones measured in two sediment cores off North Iceland in the Nordic Seas and from the subpolar gyre, South of Iceland. These records are compared with other regional proxy data from the Euro-Mediterranean region to explore the link between variations of the North Atlantic Ocean circulation and the Western Europe climate at the time where disruption of early Mediterranean civilizations was observed.

II. Material and methods

The MD99-2275 core was retrieved off North Iceland in the Western Nordic Seas (66.55°N; 17.7°W, 470 m water depth) in the vicinity of the present day polar front (Fig. 1, site 2) where the warm and salty North Icelandic Irminger Current (NIIC) meets with the cold and freshwaters of the East Icelandic Current (EIC) (Fig. 1). The age model of the MD99-2275 core is based on 7 ^{14}C dates and 2 tephras (Sicre et al., 2008; Eiríksson et al., 2011; Knudsen et al., 2008; Table 1). The second core (MD95-2015; 58.76°N; 25.95°W; 2630 m water depth) is located South of Iceland on the eastern flank of the Reikyanes Ridge (Fig. 1, site 1). Age model is based on 6 ^{14}C dates measured in planktonic foraminifera *Globigerina bulloides* (for details see Kissel et al., 2013). ^{14}C dates were calibrated using the Calib6 program and a reservoir age of 400 years (Stuiver and Reimer, 1993; Table 1). Both cores have been collected as part as the international IMAGE program.

Both sediment cores were continuously sampled at a sampling step of 1 cm for alkenone biomarker analysis. Lipids were extracted from a few grams of freeze-dried sediments following the experimental procedure described in Sicre et al. (1999). Alkenones were isolated from the total lipid extract by silica gel chromatography and quantified using a Varian CX 3400 gas chromatograph after the addition of a known amount of 5α-cholestane used as an external standard. SSTs were derived from the unsaturation index of C_{37} alkenones $U^{k'}_{37} = (C_{37:2})/(C_{37:2} + C_{37:3})$ and the calibration of Prahl et al. (1988), $T = (U^{K37} - 0.039)/0.034$). Based on the age models of the two cores, the mean temporal resolution is estimated to 4 years for MD99-2275 and 20 years for MD95-2015.

Pollen data from the KSGC-31 core (Fig. 1, site 11) were generated from 16 samples taken within the 4.2 ka time interval to obtain complementary information on vegetation changes. The pollen extraction procedure follows the standard method modified from Faegri and Iversen (1989) (for details see Combourieu-Nebout et al., 1999). In the KSGC-31 core, pollen counting was performed on least 300 grains (more than 100 if we except Pinus grains).

Clim. Past Discuss., https://doi.org/10.5194/cp-2018-159
Manuscript under review for journal Clim. Past
Discussion started: 21 November 2018

Pollen deposited at our core site originates from the large catchment area of the Gulf of Lion thus providing an integrated picture of the vegetation from the coastline to the top of the nearby mountains. Pollen percentages were calculated with respect to total pollen excluding Pinus pollen over represented in marine sediments (Combourieu-Nebout et al., 1999, 2013 and reference therein). Temperate forest pollen gathered deciduous trees mainly deciduous Quercus and Carpinus, Corylus, Fraxinus, Ulmus, Tilia, Populus, Salix... In marine records, variations of this group are commonly considered as reflecting regional changes in temperature and/or precipitation. Altitudinal conifer forest Abies (mainly) and Picea were added together. Variations of this group feature the expansion of the altitudinal forest in the region that is classically interpreted as a decrease in temperature.

III. Results and discussion

As shown in Figure 2, SST signal of the MD99-2275 core contains strong decadal scale variability with values ranging between 7 and 10 °C around a mean value of 9 °C. Within the 4.2 event interval shaded in grey, they depict an overall cooling of ~2 °C followed by a brief reversal around 4200 yr BP and an abrupt decline to coldest values reached at about 4050 yr BP. South of Iceland SSTs are warmer (above 9 °C) as expected from the core location and depict multi-centennial oscillations of broadly opposite sign of those off North Iceland with warmest SSTs peaking around 4285 yr BP.

III.1. Evidence of weak North Atlantic SPG circulation during the 4.2 ka BP event

Figure 3 compares our SST data and several records from North Atlantic sediments which includes the reconstruction of the subpolar gyre (SPG) intensity of Thornalley et al. (2009) and the mean sortable silt (SS) from Gardar drift sediments of Mjell et al. (2015) driven by the strength of the Iceland-Scotland Overflow Water (ISOW). This proxy is thought to reflect changes of the Nordic seas overflow a major component of the thermohaline circulation. Also shown are the Na fluxes from GISP2 ice core (Fig. 3e) (O'Brien et al., 1995) reflecting changes in atmospheric circulation pathways. Reconstructions of sea-ice concentration over the East Greenland shelf (Fig 3f) and sea surface salinity in the Labrador Sea (Fig. 3g) (Solignac et al., 2004; 2006) provide additional information on surface ocean circulation changes. Finally, summer SSTs derived from diatom (Fig. 3h) were used to assess variations of the Atlantic water influx into the Nordic Seas (Berner et al., 2011). These surface water property and dynamical proxy reconstructions were combined to determine North Atlantic circulation changes during the 4.2 ka BP event.

As earlier stressed, warm SSTs in the subpolar gyre region contrast with generally colder SSTs in the Nordic Seas and cold climate in Europe. Similar temperature pattern was also evidenced during the Little Ice Age (LIA), the most recent of the Holocene RCCs by Moreno-Chamarro et al. (2017). Using model simulations and proxy data these authors concluded that this temperature dipole was caused by a weakening of the SPG. A weak SPG then create the conditions for atmospheric blocking in the Northeastern Atlantic and subsequent severe climate in Europe (Häkkinen et al., 2011; Luterbacher et al., 2004). According to Moreno-Chamarro et al. (2017), the regression of the SPG would be related to solar maxima while other studies argue for solar minima as a driving factor (Barriopedro et al, 2008, Moffa-Sanchez et al., 2014). Recently, Ionita et al. (2016) demonstrated that persistent blocking activity could trigger even more rapid ocean changes such as during the Great Salinity Anomaly (GSA) in the 1970s. They showed that enhanced sea ice export from the Arctic Ocean through Fram Strait and subsequent freshening in the Labrador Sea several years later were responsible for a decrease of convection and a slowdown of the SPG. In the following, we explore the hypothesis of a reduction of the SPG and causal links between sea ice, wind intensity, SPG and AMOC to explain our results.

Figure 3c shows the reconstruction of the SPG strength based on water density difference between surface and subsurface waters obtained from paired Mg/Ca and $\delta^{18}O$ in *Globigerina. bulloides* and *Globorotalia inflata*, respectively (Thornalley et al., 2009). This density difference reflects the stratification of the upper ocean due to variable contribution of the North Atlantic Inflow and Polar waters. Lower (higher) and decreasing (increasing) values of

this index are indicative of a slowdown (strengthening) of the SPG. This index shows a gradual decrease of the SPG from 5300 yr BP to 4200-4100 yr BP. The concurrent decrease of the SS inferred ISOW intensity suggests a consistent parallel AMOC decline (Fig. 3d) (Thornalley et al., 2018) that is supported by cooling summer SST off Norway (Fig. 1, site 9 and 3h; Berner et al., 2011). All together, these reconstructions indicate a progressive slowdown of the SPG and AMOC between 5000 and 4200-4100 yr BP and subsequent northward heat transport reduction leading to cold conditions in the Nordic seas.

Freshwater export from the Arctic Ocean and wind stress are controlling factors of the SPG circulation through deep convection in the Labrador Sea (Thornalley et al., 2009). Increase sea salt Na flux in Greenland ice core has been related to the expansion of the polar vortex and/or enhance meridional wind flow. The negative trending of Na fluxes till about 4200-4300 yr BP and parallel SPG weakening are suggestive of either a weakening of the winds or more sea ice cover both acting to reduce the formation of sea salt aerosols (Fig. 3e). Proxy records of ice and melt water out the Arctic Ocean through Fram Strait during the 4.2 ka BP event are scarce. However, data from South of the Denmark Strait shown in Figure 3f, indicate that the 4500 - 3900 yr BP interval has been a long-standing period with almost no sea ice (core JM96 1207; Solignac et al., 2006). Decrease influence of Polar Waters is also evident from increasing sea surface salinity record in the Labrador Sea between 4800 and 4000 yr BP (Fig. 3g; site 5 in Fig. 1; Solignac et al., 2004). Both proxy reconstructions point to a decreased influence of Polar Waters along the East Greenland shelf since 4900 yr BP (Solignac et al., 2006; De Vernal et al., 2013). Paleodata as well as modern observations have also shown that in a weak state, the SPG is confined to the western side of the basin and has a North/South orientation favoring IC inflow waters to the SE Greenland/NW Iceland shelf (Hátún et al., 2005; Andresen et al., 2012). Such incursions of warm IC water have notably been evidenced by high occurrences of the benthic foraminifera *casidulina neotertis* between 5200 and 4200 yr BP by Andresen et al. (2012). A weak SPG also induces surface cooling in the Nordic seas due to decreased heat transport thereby promoting the expansion of sea ice cover especially in the Nordic Barents seas (Moreno-Chamarro et al., 2017). This is in agreement with the long-term cooling of Nordic Seas reported by Berner et al. (2011) along the Norwegian coast (Fig. 3h) and the marked increase abundance of sea-ice species between 4300 and 4100 yr BP in MD99-2275 that parallels the alkenone SSTs decrease (Ran et al., 2008). Note that these authors further specified that the change in Arctic species is only minor, which further supports the assumption of a low Arctic water influx and rather more local sea ice formation due to colder conditions. Sea ice concentration in the Barents Sea show consistent increasing values since 4600 yr BP (De Vernal et al., 2013) in contrast to SE Greenland and Labrador Sea, a result that is in agreement with the SST dipole distinctive imprint of SPG weakening. In the next section we discuss the climatic expression of the 4.2 ka BP event in the Euro-Mediterranean region based on continental record of concomitant hydroclimate changes.

III.2. Climatic expression in the Euro-Mediterranean region

Figure 4 shows high-resolution of SST and pollen records from the Gulf of Lion together with oxygen isotope signals from several stalagmites from the western Mediterranean sensitive to continental precipitation (Smith et al., 2016; Zanchetta et al., 2016; Ruan et al., 2016). SSTs from North Iceland (core MD99-2275) are also shown. SSTs in the Gulf of Lion reveal a ~2°C cooling between 4400 and 3800 yr BP, with two brief colder intervals around 4300 and 4100 yr BP that seems to broadly coincide with colder SSTs as well in North Iceland, yet cooling at 4100 yr BP off North Iceland is more prominent possibly due to the presence of sea ice (Fig. 4a, c). Coldest SSTs in this area during the LIA have been related to persistent wintertime atmospheric blocking over the NE Atlantic resulting in more intense and colder Mistral winds blowing more strongly during the winter season (Sicre et al., 2016).

Pollen data at this site also indicate colder conditions over adjacent continent. Temperate forest changes closely follows the SST cooling from 4400 to 3600 yr BP (Fig. 4a, b) with several peaks superimposed on the general decreasing trend (~60 to 30%) associated with opposite increasing altitudinal conifer forest (~10 to 20%). Pollen data from the nearby Palavasian lagoon system (Azuara et al., 2018) are also consistent with pollen data in the Gulf

of Lion core. They notably display a decrease of the temperate forest and increase of altitudinal forest taxon *Fagus*. These regional vegetation changes indicate colder conditions but not necessary dryer climate since mountain forests require relative high precipitations (<750 mm). Nevertheless, on shorter time scale, the decreases of temperate forest pollen could indicate a slight and brief decrease in precipitation and thus moderate dryness and/or the establishment and lengthening of summer dryness that is typical of Mediterranean precipitation regime. This is confirmed by the concurrent enhanced representation of the Mediterranean taxa (Combourieu-Nebout pers.com).

Paleoclimatic and paleoenvironmental records from the western Mediterranean (Italy, Spain and Algeria) give different picture of precipitation during the 4.2 ka BP event. The oxygen isotope record from the Renella Cave stalagmite (Fig. 4e; Zanchetta et al., 2016) indicates dryness in central Italy between 4300-3800 yr BP. Pollen record from Adriatic Sea core MD 90-917 further support that Mediterranean precipitation regime established at that time (Combourieu-Nebout et al., 2013) while in central Italy and in Gulf of Lion, pollen data do not show a clear change in vegetation but only a modification of the forest composition that can be accounted by a slight decrease in precipitation (Di Rita et al., 2018; this issue). Stable oxygen isotopes and archaeological data from Gueldaman cave in northern Algeria indicate dry conditions and subsequent abandonment of the cave between 4400-3800 yr BP similar to Renella Cave (Fig. 4f; Ruan et al., 2016). Quite different, the Asiul Cave record from Northern Spain in the Atlantic realm (Fig. 4d) shows multi-decadal scale variability with cold and dry intervals (down arrows) that share resemblance with the cold spell found in the Nordic Seas and Gulf of Lion SST records (Smith et al., 2016). Deflected westerly wind flow to the North under frequent blocked regimes could account for less humid conditions in North Iberia (Hakkinen et al., 2011). Stable oxygen isotopes from Renella and Gueldaman caves indicate concurrent departure to wetter conditions (up arrows) indicative of other atmospheric influences that would need further investigations.

In summary, our reconstructions all together show that from 4400 to 3800 yr BP the region experienced colder and drier climate most likely triggered by a weakening of the North Atlantic SPG under sustained high solar activity (Kobashi et al., 2017). In line with the study of Moreno-Chamarro et al. (2017) we hypothesize that during the 4.2 event, the SPG was also weakened and responsible for cold and slightly drier climate in Northwestern Europe and in the Nordic Seas, contrasting with a warmer subpolar North Atlantic. Figure 5 shows the SST dipole of a weak SPG from Moreno-Chamarro et al. (2017) obtained from model simulation during the LIA together with the data used in the discussion represented by colored dots. Anomalies for the 4.2 ka BP event were calculated with respect to the period between 5000 and 4400 yr BP. Red (blue) dots indicate positive (negative) SST/air temperature anomalies while open orange dots highlight negative humidity anomalies.

IV. Conclusions

Unprecedented high-resolution alkenone-derived SST records of the 4.2 ka BP event have been generated from the Nordic Seas and North Atlantic sediments in order to explore causes for this cold/dry event of the mid-Holocene considered as the onset of the neoglacial period in the North Atlantic and the role of the ocean in the observed changes. The spatial distribution of the SST indicates a cold/warm dipole between 4400 and 4100 yr BP that characterize a weak subpolar gyre circulation which is supported by other marine proxy records across the North Atlantic. Enhanced wintertime atmospheric blocking induced by a weak subpolar gyre circulation would account for the hydroclimate changes seen in the available continental proxy record in the Euro-Mediterranean region. The high solar activity and absence of major volcanic activity during this period could have promoted this dynamical change of the SPG.

Acknowledgments

This work was financially supported by the MISTRALS/PaleoMex program. The research leading to this study has received funding from the French National Research Agency HAMOC project (ANR-13-BS06- 0003). We thank Sandrine Canals for the pollen samples processing performed at ISEM laboratory in Montpellier.

References

Andresen, C. S., Hansen, M. J., Seidenkrantz, M. S., Jennings, A. E., Knudsen, M. F., Nørgaard-Pedersen, N., ... & Pearce, C.: Mid-to late-Holocene oceanographic variability on the Southeast Greenland shelf, The Holocene, 23(2), 167-178, 2012.

Azuara, J., Lebreton, V., Peyron, O., Mazier, F., & Combourieu-Nebout, N.: The Holocene history of low altitude Mediterranean Fagus sylvatica forests in southern France, Journal of Vegetation Science, 29(3), 438-449, 2018.

Barriopedro, D., García-Herrera, R., & Huth, R.: Solar modulation of Northern Hemisphere winter blocking, Journal of Geophysical Research: Atmospheres, 113(D14), 2008.

Berkelhammer M. Sinha A. Stott L. Cheng H. Pausata F.S.R. Yoshimura K.: An abrupt shift in the Indian monsoon 4000 years ago, in Giosan L.et al. ., eds., Climates, landscapes, and civilizations: American Geophysical Union Geophysical Monograph 198 , p. 75–87, doi:10.1029/2012GM001207, 2012.

Berner, K. S., Koç, N., Godtliebsen, F., & Divine, D.: Holocene climate variability of the Norwegian Atlantic Current during high and low solar insolation forcing, Paleoceanography and Paleoclimatology, 26(2), 2011.

Bond, G., Kromer, B., Beer, J., Muscheler, R., Evans, M. N., Showers, W., & Bonani, G.: Persistent solar influence on North Atlantic climate during the Holocene, Science, 294(5549), 2130-2136, 2001.

Booth, R. K., Jackson, S. T., Forman, S. L., Kutzbach, J. E., Bettis III, E. A., Kreig, J., and Wright, D. K.: A severe centennial-scale drought in mid-continental North America 4200 years ago and apparent global linkage, The Holocene, 15, 321-328, 2005.

Bronk Ramsey, C.: Development of the radiocarbon program OxCal, Radiocarbon 43, 355–363, 2001.

Cheng, H., Sinha, A., Verheyden, S., Nader, F. H., Li, X. L., Zhang, P. Z., ... & Ning, Y. F.: The climate variability in northern Levant over the past 20,000 years, Geophysical Research Letters, 42(20), 8641-8650, 2015.

Combourieu-Nebout, N, Londeix, L, Baudin, F.: Quaternary marine and continental paleoenvironments in the western Mediterranean (Site 976, Alboran Sea): Palynological evidence: In Zahn, R, Comas, MC, Klaus, A (eds) Proceedings of ODP Scientific Results, vol. 161. College Station, TX: Ocean Drilling Program, 457–468, 1999.

Combourieu-Nebout, N., Peyron, O., Bout-Roumazeilles, V., Goring, S., Dormoy, I., Joannin, S., Sadori, L., Siani, G., and Magny, M.: Holocene vegetation and climate changes in the central Mediterranean inferred from a high-resolution marine pollen record (Adriatic Sea), Clim. Past, 9, 2023-2042, https://doi.org/10.5194/cp-9-2023-2013, 2013.

De Vernal, A., Hillaire-Marcel, C., Rochon, A., Fréchette, B., Henry, M., Solignac, S., & Bonnet, S.: Dinocyst-based reconstructions of sea ice cover concentration during the Holocene in the Arctic Ocean, the northern North Atlantic Ocean and its adjacent seas, Quaternary Science Reviews, 79, 111-121, 2013.

Di Rita, F. and Magri, D.: The 4.2 ka BP event in the vegetation record of the central Mediterranean, Clim. Past Discuss., https://doi.org/10.5194/cp-2018-128, in review, 2018.

Dixit, Y., Hodell, D. A., & Petrie, C. A.: Abrupt weakening of the summer monsoon in northwest India~ 4100 yr ago. Geology, 42(4), 339-342, 2014.

Donges, J. F., Donner, R., Marwan, N., Breitenbach, S. F., Rehfeld, K., & Kurths, J.: Non-linear regime shifts in Holocene Asian monsoon variability: potential impacts on cultural change and migratory patterns, Climate of the Past, 11(5), 709-741, 2015.

Eiríksson, J., Knudsen, K. L., Larsen, G., Olsen, J., Heinemeier, J., Bartels-Jónsdóttir, H. B., ... & Símonarson, L. A.: Coupling of palaeoceanographic shifts and changes in marine reservoir ages off North Iceland through the last millennium, Palaeogeography, Palaeoclimatology, Palaeoecology, 302(1-2), 95-108, 2011.

Faegri, K. and Iversen, J.: Textbook of pollen analysis, 4th Edn., edited by: Faegri, K., Kaland, P. E., and Krzywinski, K., Wiley, Chichester, 1989.

Finné, M., Holmgren, K., Shen, C. C., Hu, H. M., Boyd, M., & Stocker, S.: Late Bronze Age climate change and the destruction of the Mycenaean Palace of Nestor at Pylos, PloS one, 12(12), e0189447, 2017.

Fisher, D., Osterberg, E., Dyke, A., Dahl-Jensen, D., Demuth, M., Zdanowicz, C., ... & Kreutz, K.: The Mt Logan Holocene—late Wisconsinan isotope record: tropical Pacific—Yukon connections, The Holocene, 18(5), 667-677, 2008.

Fohlmeister, J., Vollweiler, N., Spötl, C., & Mangini, A.: COMNISPA II: Update of a mid-European isotope climate record, 11 ka to present, The Holocene, 23(5), 749-754, 2013.

Häkkinen, S., Rhines, P. B., & Worthen, D. L.: Atmospheric blocking and Atlantic multidecadal ocean variability, Science, 334(6056), 655-659, 2011.

Hátún, H., Sandø, A. B., Drange, H., Hansen, B., & Valdimarsson, H.: Influence of the Atlantic subpolar gyre on the thermohaline circulation, Science, 309(5742), 1841-1844, 2005.

Ionita, M., Scholz, P., Lohmann, G., Dima, M., & Prange, M.: Linkages between atmospheric blocking, sea ice export through Fram Strait and the Atlantic Meridional Overturning Circulation, Scientific reports, 6, 32881, 2016.

Jalali B, Sicre MA, Bassetti MA et al.: Holocene climate variability in the North-Western Mediterranean Sea (Gulf of Lions), Climate of the past 12: 91–101, 2016.

Kissel, C., Van Toer, A., Laj, C., Cortijo, E., & Michel, E. : Variations in the strength of the North Atlantic bottom water during Holocene, Earth and Planetary Science Letters, 369, 248-259, 2013.

Knudsen, K. L., Søndergaard, M. K. B., Eiríksson, J., & Jiang, H.: Holocene thermal maximum off North Iceland: Evidence from benthic and planktonic foraminifera in the 8600–5200 cal year BP time slice, Marine Micropaleontology, 67(1), 120-142, 2008.

Kobashi, T., Menviel, L., Jeltsch-Thömmes, A., Vinther, B. M., Box, J. E., Muscheler, R., ... & Wanner, H.: Volcanic influence on centennial to millennial Holocene Greenland temperature change, Scientific reports, 7(1), 1441, 2017.

Liu, F., & Feng, Z.: A dramatic climatic transition at~ 4000 cal. yr BP and its cultural responses in Chinese cultural domains, The Holocene, 22(10), 1181-1197, 2012.

Liu, Z., Yoshimura, K., Bowen, G. J., Buenning, N. H., Risi, C., Welker, J. M., and Yuan, F.: Paired oxygen isotope records reveal modern North American atmospheric dynamics during the Holocene, Nature Communications, 5, 3701, DOI: 10.1038/ncomms4701, 2014.

Locarnini, R. A., Mishonov, A. V., Antonov, J. I., Boyer, T. P., Garcia, H. E., Baranova, O. K., et al. : In S. Levitus (Ed.), technical ed A Mishonov World Ocean Atlas 2013, Volume 1: Temperature (Vol. 73, p. 40). MD: NOAA Atlas NESDIS. Retrieved from http://www.nodc.noaa.gov/OC5/indprod.html, 2013.

Luterbacher, J., Dietrich, D., Xoplaki, E., Grosjean, M., & Wanner, H.: European seasonal and annual temperature variability, trends, and extremes since 1500, Science, 303(5663), 1499-1503, 2004.

Magny, M., Combourieu-Nebout, N., De Beaulieu, J. L., Bout-Roumazeilles, V., Colombaroli, D., Desprat, S., ... & Revel, M.: North-south palaeohydrological contrasts in the central Mediterranean during the Holocene: tentative synthesis and working hypotheses, Climate of the Past, 9, 2043-2071, 2013.

Mayewski, P. A., Rohling, E. E., Stager, J. C., Karlén, W., Maasch, K. A., Meeker, L. D., ... & Lee-Thorp, J.: Holocene climate variability, Quaternary research, 62(3), 243-255, 2004.

McDermott, F., Mattey, D. P., & Hawkesworth, C.: Centennial-scale Holocene climate variability revealed by a high-resolution speleothem δ18O record from SW Ireland, Science, 294(5545), 1328-1331, 2001.

Mjell, T. L., Ninnemann, U. S., Eldevik, T., & Kleiven, H. K. F., Holocene multidecadal-to millennial-scale variations in Iceland-Scotland overflow and their relationship to climate, Paleoceanography, 30(5), 558-569, 2015.

Moffa-Sánchez, P., Born, A., Hall, I. R., Thornalley, D. J., & Barker, S.: Solar forcing of North Atlantic surface temperature and salinity over the past millennium, Nature Geoscience, 7(4), 275, 2014.

Moreno-Chamarro, E., Zanchettin, D., Lohmann, K., Luterbacher, J., & Jungclaus, J. H.: Winter amplification of the European Little Ice Age cooling by the subpolar gyre, Scientific Reports, 7(1), 9981, 2017.

Nakamura, A., Yokoyama, Y., Maemoku, H., Yagi, H., Okamura, M., Matsuoka, H., ... & Ikehara, M.: Weak monsoon event at 4.2 ka recorded in sediment from Lake Rara, Himalayas, Quaternary International, 397, 349-359, 2016.

Ning, L., Liu, J., Bradley, R. S., and Yan, M.: Comparing the spatial patterns of climate change in the 9th and 5th millennia B.P. from TRACE-21 model simulations, Clim. Past Discuss., https://doi.org/10.5194/cp-2018-132, in review, 2018.

O'Brien, S. R., Mayewski, P. A., Meeker, L. D., Meese, D., Twickler, M. S., & Whitlow, S. I.: Complexity of Holocene climate as reconstructed from a Greenland ice core, Science, 270(5244), 1962-1964, 1995.

Prahl, F.G., Muehlhausen, L.A., Zahnle, D.L.: Further evaluation of longchain alkenones as indicators of paleoceanographic conditions, Geochim. Cosmochim. Acta 52, 2303–2310, 1988.

Ran, L., Jiang, H., Knudsen, K. L., & Eiriksson, J.: A high-resolution Holocene diatom record on the North Icelandic shelf, Boreas, 37(3), 399-413, 2008.

Ruan, J., Kherbouche, F., Genty, D., Blamart, D., Cheng, H., Dewilde, F., ... & Michelot, J. L.: Evidence of a prolonged drought ca. 4200 yr BP correlated with prehistoric settlement abandonment from the Gueldaman GLD1 cave, Northern Algeria, Climate of the Past, 12(1), 1-14, 2016.

Sicre, M. A., Jacob, J., Ezat, U., Rousse, S., Kissel, C., Yiou, P., ... & Turon, J. L.: Decadal variability of sea surface temperatures off North Iceland over the last 2000 years, Earth and Planetary Science Letters, 268(1-2), 137-142, 2008.

Sicre, M. A., Jalali, B., Martrat, B., Schmidt, S., Bassetti, M. A., & Kallel, N.: Sea surface temperature variability in the North Western Mediterranean Sea (Gulf of Lion) during the Common Era, Earth and Planetary Science Letters, 456, 124-133, 2016.

Sicre, M. A., Ternois, Y., Miquel, J. C., & Marty, J. C.: Alkenones in the Northwestern Mediterranean sea: interannual variability and vertical transfer, Geophysical Research Letters, 26(12), 1735-1738, 1999.

Smith, A. C., Wynn, P. M., Barker, P. A., Leng, M. J., Noble, S. R., & Tych, W.: North Atlantic forcing of moisture delivery to Europe throughout the Holocene, Scientific reports, 6, 24745, 2016.

Solignac, S., de Vernal, A., & Hillaire-Marcel, C.: Holocene sea-surface conditions in the North Atlantic—contrasted trends and regimes in the western and eastern sectors (Labrador Sea vs. Iceland Basin), Quaternary Science Reviews, 23(3-4), 319-334, 2004.

Solignac, S., Giraudeau, J., & de Vernal, A.: Holocene sea surface conditions in the western North Atlantic: spatial and temporal heterogeneities, Paleoceanography, 21(2), 2006.

Stanley J, Krom M, Cliff R et al.: Nile flow failure at the end of the Old Kingdom, Egypt: Strontium isotopic and petrologic evidence, Geoarchaeology 18: 395–402, 2003.

Stuiver, M., & Reimer, P. J.: Extended 14 C data base and revised CALIB 3.0 14 C age calibration program, Radiocarbon, 35(1), 215-230, 1993.

Stuiver, M., Braziunas, T.F.: Modeling atmospheric 14C influences and 14C ages of marine samples to 10,000 BC. In: Stuiver, M., Long, A., Kra, R.S. (Eds.), Calibration 1993, Radiocarbon, vol. 35, pp. 137–189, 1993.

Thornalley, D. J., Elderfield, H., & McCave, I. N.: Holocene oscillations in temperature and salinity of the surface subpolar North Atlantic, Nature, 457(7230), 711, 2009.

Thornalley, D. J., Oppo, D. W., Ortega, P., Robson, J. I., Brierley, C. M., Davis, R., ... & Yashayaev, I.: Anomalously weak Labrador Sea convection and Atlantic overturning during the past 150 years, Nature, 556(7700), 227, 2018.

Walker, M.J., Berkelhammer, M., Björck, S., Cwynar, L.C., Fisher, D.A., Long, A.J., Lowe, J.J., Newnham, R.M., Rasmussen, S.O. and Weiss, H.: Formal subdivision of the Holocene Series/Epoch: a Discussion Paper by a Working Group of INTIMATE (Integration of ice-core, marine and terrestrial records) and the Subcommission on Quaternary Stratigraphy (International Commission on Stratigraphy), Journal of Quaternary Science, 27, 649-659, 2012.

Wanner, H., Mercolli, L., Grosjean, M., & Ritz, S. P.: Holocene climate variability and change; a data-based review. Journal of the Geological Society, 172(2), 254-263, 2014.

Wanner, H., Solomina, O., Grosjean, M., Ritz, S. P., & Jetel, M.: Structure and origin of Holocene cold events, Quaternary Science Reviews, 30(21-22), 3109-3123, 2011.

Weiss, H., & Bradley, R. S.: What drives societal collapse?, Science, 291(5504), 609-610, 2001.

Weiss, H.: Global megadrought, societal collapse and resilience at 4.2-3.9 ka BP across the Mediterranean and west Asia, PAGES Magazine, 24, 62-63, 2016.

Weiss, H.: Megadrought, collapse, and resilience in late 3rd millennium BC Mesopotamia. In book: Meller, H., Arz, H. W., Jung, R., and Risch, R., eds, 2200 BC – A climatic breakdown as a cause for collapse of the Wold World? Halle: Landesmuseum fur Vorgeschichte, 35-52, 2015.

Zanchetta, G., Regattieri, E., Isola, I., Drysdale, R. N., Bini, M., Baneschi, I., & Hellstrom, J. C.: The so-called “4.2 event” in the central Mediterranean and its climatic teleconnections, Alp Mediterr Quat, 29, 5-17, 2016.

Clim. Past Discuss., https://doi.org/10.5194/cp-2018-159
Manuscript under review for journal Clim. Past
Discussion started: 21 November 2018

Table 1: Age models of the MD95-2015 and MD99-2275 sediment cores (from Kissel et al., 2013; Knudsen et al., 2008). Radiocarbon ages have been calibrated using CALIB6 program with a reservoir age of 400 years, for core MD95-2015 (Stuiver and Reimer, 1993), and using OxCal3.1 (Bronk Ramsey, 2001) and the Marine04 model calibration curve (Stuiver and Braziunas, 1993), for core MD99-2275.

Core	Depth (cm)	Material/Dated tephra layer	^{14}C Ages	Error (1sigma)	Cal year BP	Error (1sigma)
MD95-2015	60	G. bulloides	2220	60	1810	72
MD95-2015	90	G. bulloides	2960	60	2736	33
MD95-2015	110	G. bulloides	3390	60	3263	71
MD95-2015	150	G. bulloides	4060	60	4070	86
MD95-2015	200	G. bulloides	4660	70	4886	72
MD95-2015	240	G. bulloides	5310	80	5662	77
MD99-2275	687	Hekla 3			2980	0
MD99-2275	942	Hekla 4			4200	0
MD99-2275	9695	Siphonodentalium lobatum	4405	45	4565	85
MD99-2275	10020	Thyasira equalis	4760	100	5030	160
MD99-2275	10455	Yoldiella lenticula	4805	65	5100	120
MD99-2275	10675	Thyasira equalis	4880	60	5185	105
MD99-2275	10885	Thyasira equalis	5160	80	5520	90
MD99-2275	11545	Thyasira equalis	5105	50	5490	70
MD99-2275	12325	Yoldiella cf. lenticula	5500	50	5880	70

Figure captions

Figure 1: Map of the annual mean SSTs (1955–2012) from World Ocean Atlas database (https://data.nodc.noaa.gov/las/getUI.do; Locarnini et al., 2013) showing the location of the investigated cores and sites used for comparison. (1) marine core MD95-2015 (this study); (2) marine core MD99-2275 (this study); (3) marine core GS06-144 08GC (Mjell et al., 2015); (4) marine core RAPiD-12-1K (Thornalley et al., 2009); (5) marine core P-013 (Solignac et al., 2004); (6) marine core JM96 1207 (Solignac et al., 2006); (7) ice core GISP2 (O'Brien et al., 1995); (8) marine core Fox05R/04G (Andresen et al., 2012); (9) marine core MD95-2011 (Berner et al., 2011); (10) Crag Cave (McDermott et al., 2001); (11) marine core KSGC-31 (Jalali et al., 2016; this study); (12) Palavasian Lagoon (Azuara et al., 2015); (13) speleothem from Asiul Cave (Smith et al., 2016); (14) speleothem from Renella Cave (Zanchetta et al., 2016); (15) speleothem from Gueldaman Cave (Ruan et al., 2016). Subpolar and subtropical gyres as well as main surface currents in the North Atlantic are also shown. IC: Irminger Current; NIIC: North Icelandic Irminger Current; EIC: East Icelandic Current; EGC: East Greenland Current.

Figure 2: Sea surface temperatures (SSTs) in the North Atlantic between 5500 and 2500 yr BP. (a) Alkenone-derived SSTs at the MD95-2015 core (site 1 in Fig. 1). (b) Alkenone-derived SSTs at the MD99-2275 core (site 2 in Fig. 1). 50 years binning is applied to reduce the effect of proxy reconstruction error (thick lines). Triangles indicate the age control points used for the age models, at 1σ uncertainty for the ^{14}C dates.

Figure 3: Paleoclimatic and paleoceanographic data from the North Atlantic during the 4.2 ka BP event. (a) Alkenone-derived SSTs at the MD95-2015 core. (b) Alkenone-derived SSTs at the MD99-2275 core. (c) Density difference between surface and subsurface waters obtained from paired Mg/Ca and $\delta^{18}O$ in *Globigerina bulloides* and *Globorotalia inflata* in ore RAPiD-12-1K (site 4 in Fig. 1) (Thornalley et al., 2009). (d) Mean sortable silt (SS) in core GS06-144 08GC in the Iceland Basin (site 3 in Fig. 1) inferred Iceland-Scotland Overflow Water flow vigor (ISOW; Mjell et al., 2015). (e) Sea-salt Na flux from GISP2 ice core (site 7 in Fig. 1) (O'Brien et al., 1995). (e) Sea ice concentration from the East Greenland shelf based on dinoflagellate cyst assemblages in core JM96 1207 (site 6 in Fig. 1) (Solignac et al., 2006). (g) Dinoflagellate cyst assemblages inferred sea surface salinity from the Labrador Sea core P-013 (site 5 in Fig. 1) (Solignac et al., 2004). (h) Summer SSTs derived from diatom based weighted averaging partial least squares transfer function from core MD95-2011 (site 9 in

Fig.1) (Berner et al., 2011). For (a), (b) and (d) 50 years binning is applied to reduce the effect of proxy reconstruction error (thick lines). This binning has not been applied on the low temporal resolution records. The shaded grey vertical band represents the 4.2 ka BP event time-interval.

Figure 4: Climatic expression of the 4.2 ka BP event in the W Mediterranean region as recorded by marine and continental archives. (a) Alkenone SSTs at the KSGC-31 core in the Gulf of Lion (site 11 in Fig. 1, Jalali et al., 2016). (b) Temperate forest (yellow line) and altitudinal conifer (green line) forest pollen percentages in the KSGC-31 core (this study). (c) Alkenone SSTs at the MD99-2275 core (site 2 in Fig. 1) (North Iceland; this study). (d) Detrended $\delta^{18}O$ obtained from Asiul Cave (site 13 in Fig. 1) (North Spain; Smith et al., 2016). (e) $\delta^{18}O$ obtained from Renella Cave (site 14 in Fig. 1) (North Italy; Zanchetta et al., 2016). (f) $\delta^{18}O$ obtained from Gueldaman Cave (site 15 in Fig. 1) (North Algeria; Ruan et al., 2016). 50 years binning is applied to reduce the effect of proxy reconstruction error (thick lines). The shaded grey vertical band represents the 4.2 ka BP event time-interval.

Figure 5: Map of the North Atlantic showing the dipole SSTs related to reduced SPG circulation during the LIA (1575-1724 CE) (from Moreno-Chamarro et al., 2017). Climatic conditions during the 4400-3800 yr BP time-interval at oceanic and continental sites discussed in the text are shown by colored circles. (1) Core MD95-2015 (site 1 in Fig. 1) (this study). (2) Core MD99-2275 (site 2 in Fig. 1, This study). (3) Core Fox05R/04G (site 8 in Fig. 1, Andresen et al., 2012). (4) Crag Cave (site 10 in Fig. 1, McDermott et al., 2001). (5) Core MD95-2011 (site 9 in Fig. 1, Berner et al., 2011). (6) Core KSGC-31 (site 11 in Fig. 1, Jalali et al., 2016; This study). (7) Asiul Cave (site 13 in Fig. 1, Smith et al., 2016). (9) Renella Cave (site 14 in Fig. 1, Zanchetta et al., 2016). (10) Gueldaman Cave (site 15 in Fig. 1, Ruan et al., 2016).

Clim. Past Discuss., https://doi.org/10.5194/cp-2018-159
Manuscript under review for journal Clim. Past
Discussion started: 21 November 2018

Climate of the Past
Discussions
Open Access
EGU

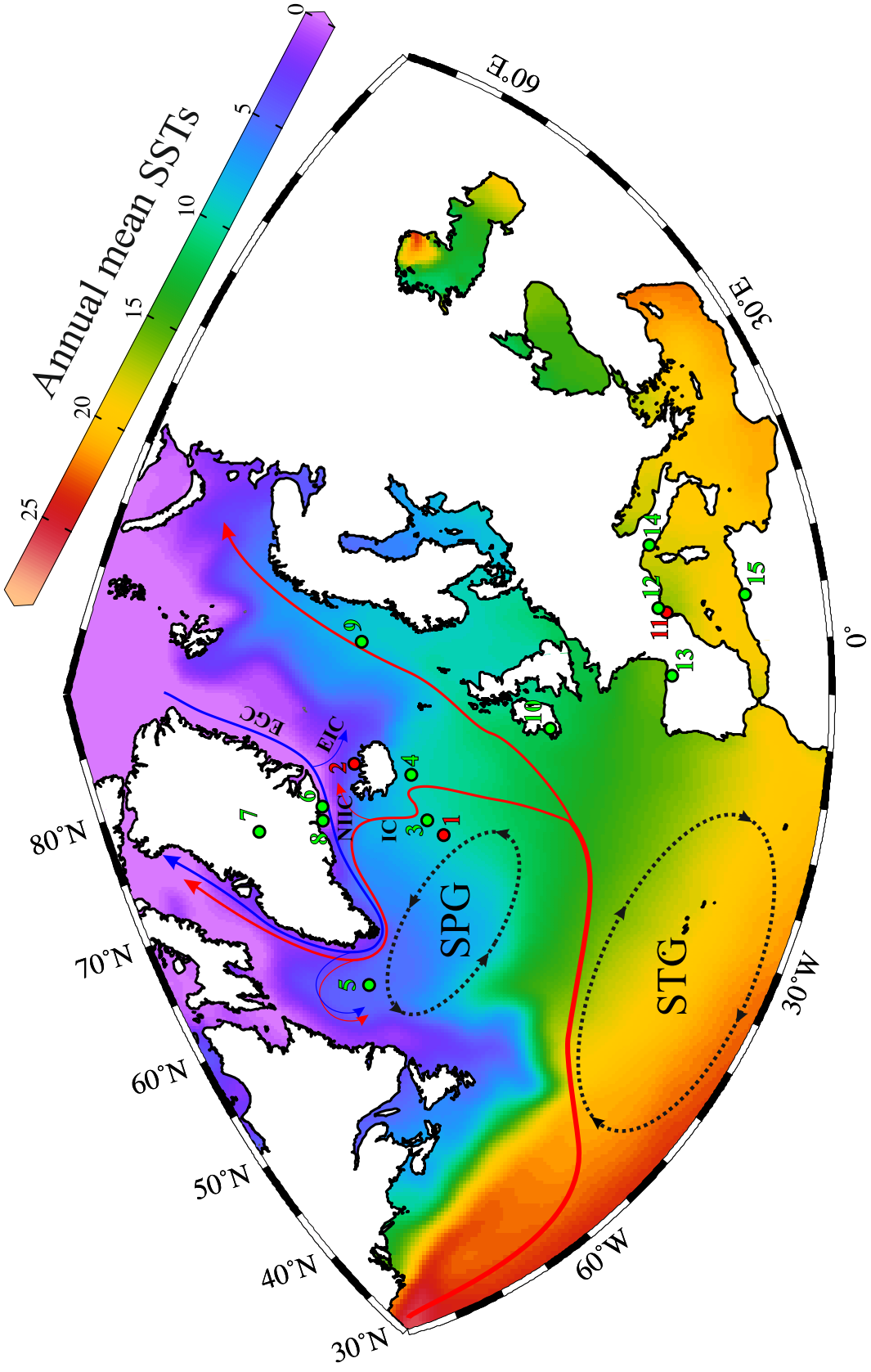

Figure 1

Clim. Past Discuss., https://doi.org/10.5194/cp-2018-159
Manuscript under review for journal Clim. Past
Discussion started: 21 November 2018

Climate of the Past
Discussions
Open Access
EGU

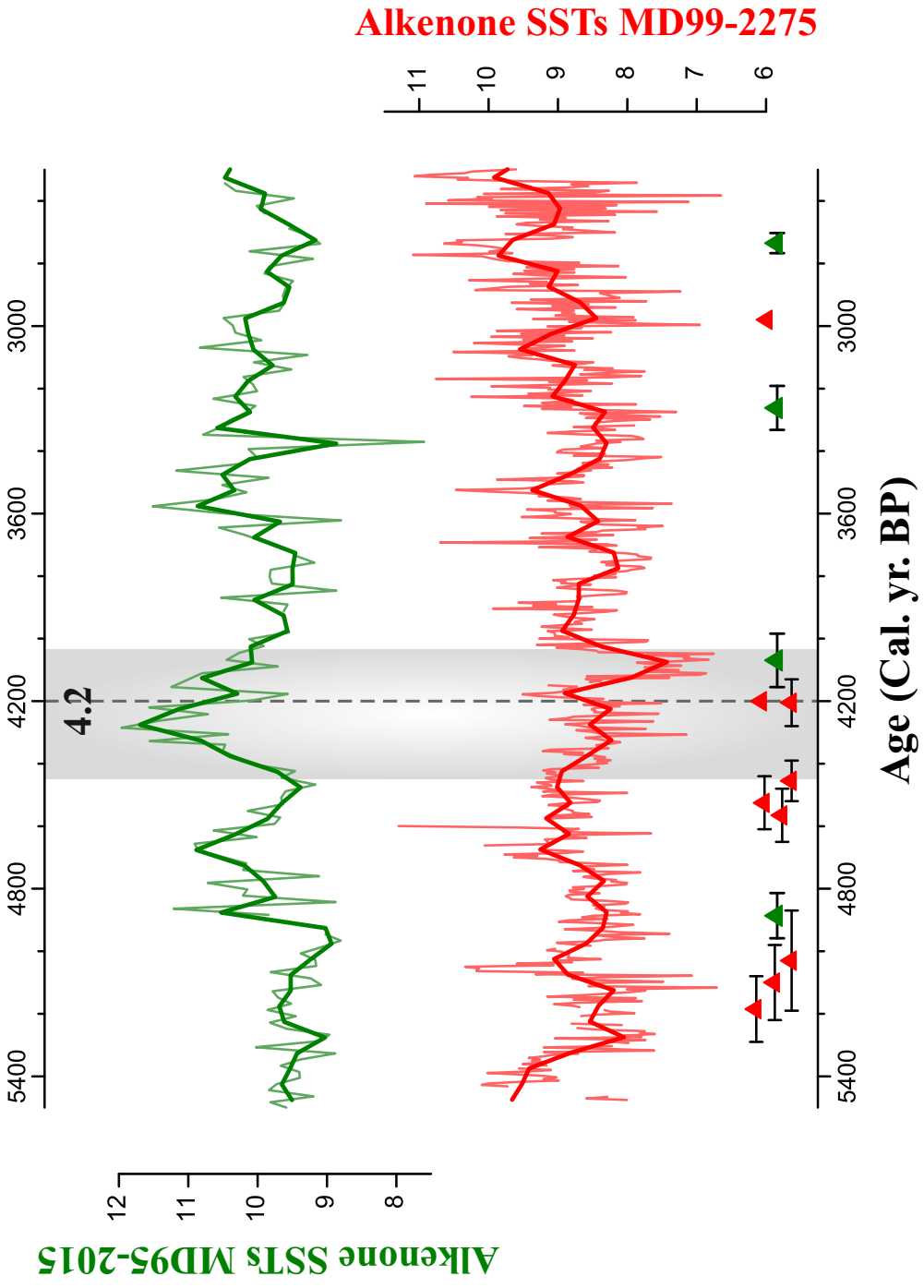

Figure 2

Clim. Past Discuss., https://doi.org/10.5194/cp-2018-159
Manuscript under review for journal Clim. Past
Discussion started: 21 November 2018

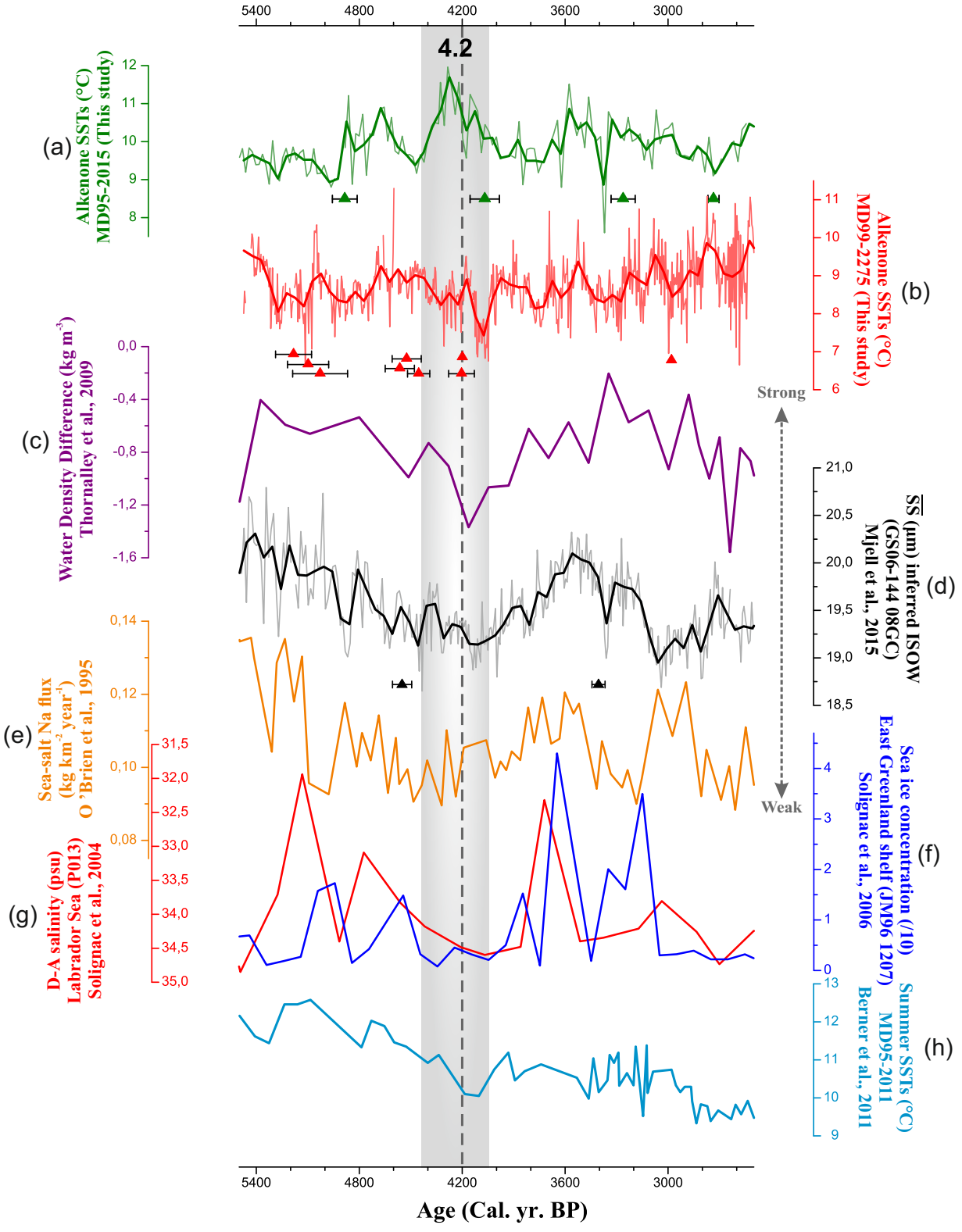

Figure 3

Clim. Past Discuss., https://doi.org/10.5194/cp-2018-159
Manuscript under review for journal Clim. Past
Discussion started: 21 November 2018

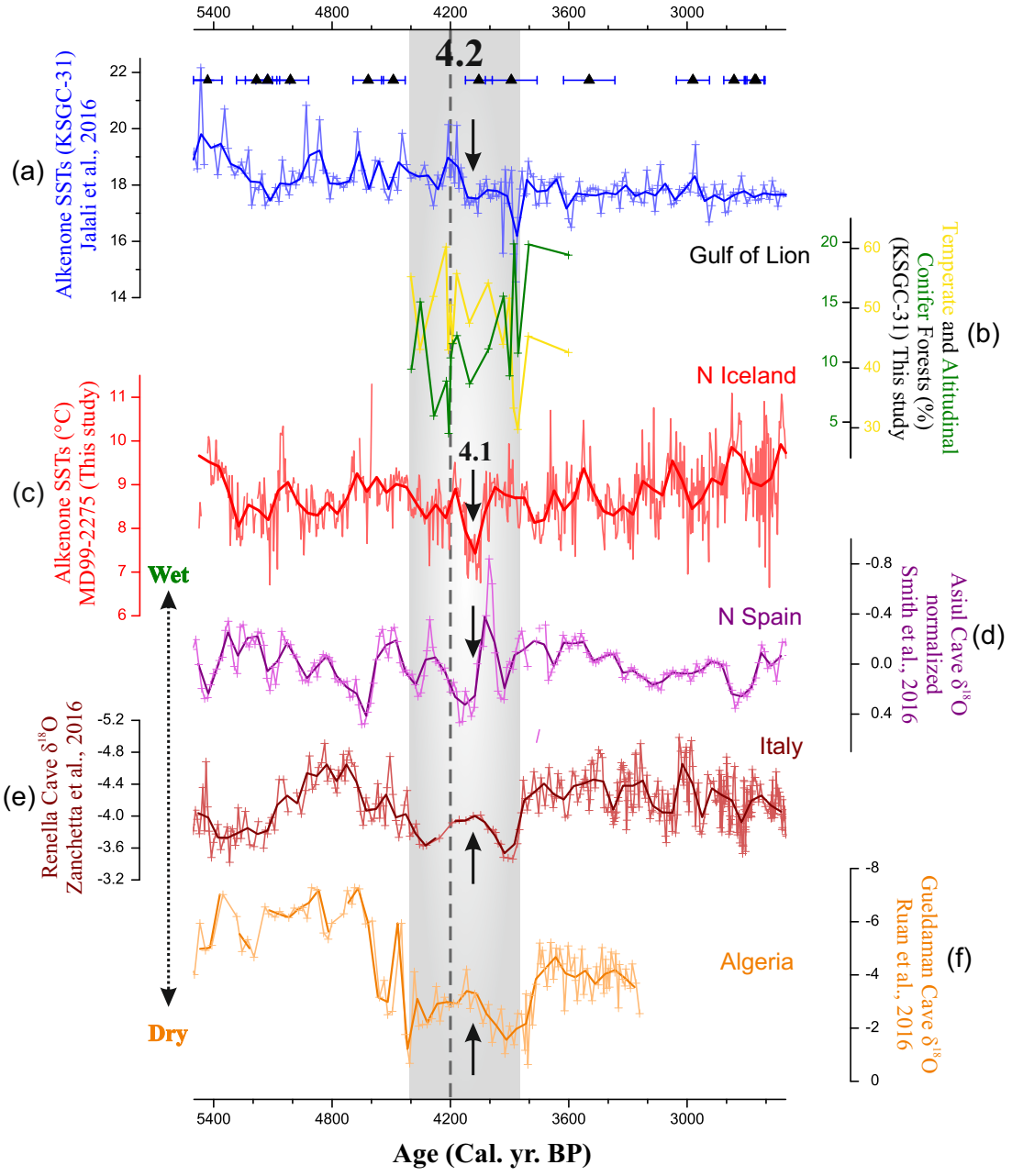

Figure 4

Clim. Past Discuss., https://doi.org/10.5194/cp-2018-159
Manuscript under review for journal Clim. Past
Discussion started: 21 November 2018

Climate of the Past
Discussions
Open Access
EGU

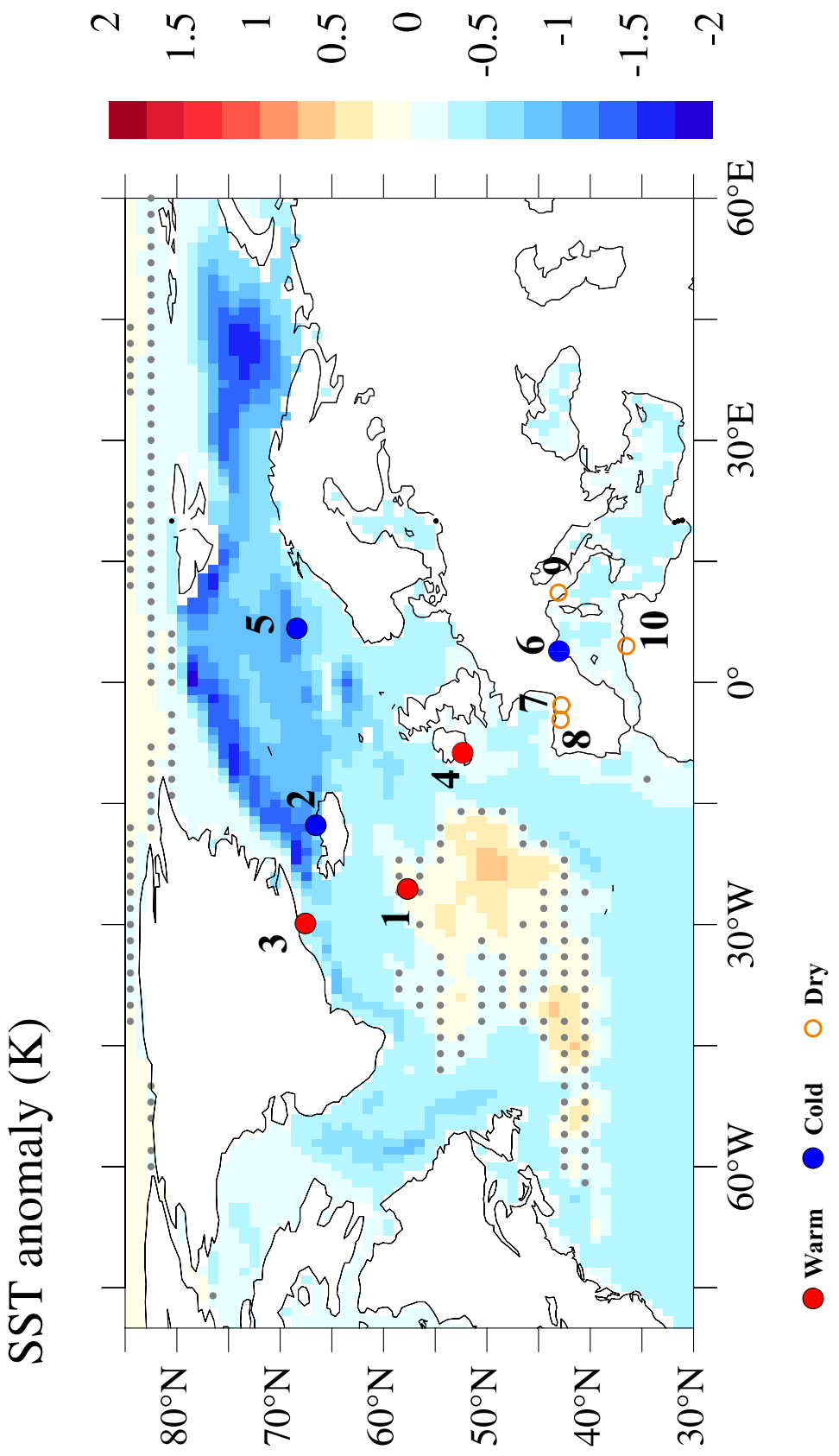

Figure 5